Mark Philip Roach - Thesis Defence

Committee Members:
Mark Iwen[1*] Longxiu Huang[1] Ekaterina Rapinchuk[1] Guowei Wei[2]

Thursday 20th April, 2023

[*] Dissertation/Thesis Director
[1] Department of Mathematics, CMSE, MSU
[2] Department of Mathematics, Biochemistry & Molecular Biology, Electrical and Computer Engineering, MSU

Table of Contents

Near-field Ptychography

- Ptychography is a particular form of masked phase retrieval in which the collections of masks are generated by taking one physical mask and shifting it in space
- Near-field Ptychography is when the distance between the lens, object, and detector are small (microscopic imaging).

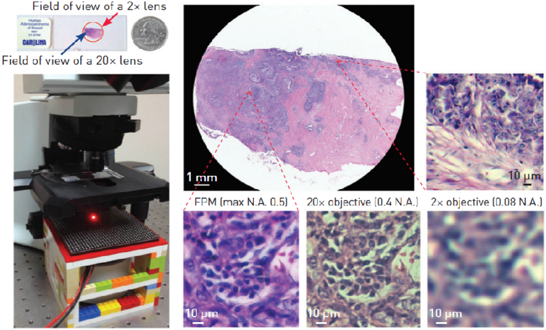

Figure: "Wide-field, high-resolution Fourier ptychographic microscopy" - G. Zheng et al., 2013

Near-field Ptychographic Measurements

- Let $\mathbf{x} \in \mathbb{C}^d$ denote the unknown object
- Let $\mathbf{m}$ denote the known mask, $\mathbf{p}$ the known point spread function (PSF).
- The noisy near-field ptychographic measurements will be of the form

$$Y_{k,\ell} = |(\mathbf{p} * (S_k \mathbf{m} \circ \mathbf{x}))_\ell|^2 + N_{k,\ell}, \quad (k,\ell) \in \mathcal{K} \times \mathcal{L} \subseteq [d] \times [d]$$

- $\mathcal{K}$: set of shifts, $\mathcal{L}$: set of frequencies
- Circular shift: $(S_k \mathbf{m})_n = m_{n+k \text{ mod } d}$
- Discrete convolution: $(\mathbf{u} * \mathbf{v})_n = \sum_{k=0}^{d-1} u_k v_{n-k \text{ mod } d}$
- Pointwise (Hadamard) product: $(\mathbf{u} \circ \mathbf{v})_n = u_n v_n$

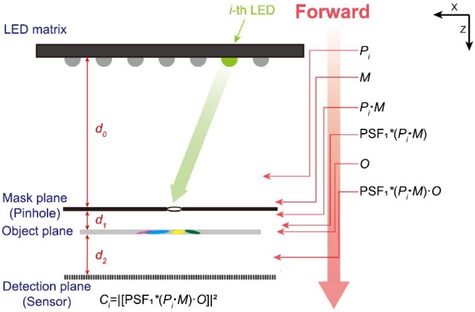

Reducing To Inner Product Form

- Consider the noiseless measurements $Y_{k,\ell} = |(\mathbf{p} * (S_k\mathbf{m} \circ \mathbf{x}))_\ell|^2, \ (k,\ell) \in [d] \times [2\delta - 1]$
- By letting $Y_{k,\ell} = Y_{-k,\ell+k}, \check{\mathbf{m}}_\ell^{(p,m)} = \overline{S_\ell \tilde{\mathbf{p}} \circ \mathbf{m}}, (\tilde{p})_n = p_{-n}$, one can show that
$$Y_{k,\ell} = |\langle \check{\mathbf{m}}_\ell^{(p,m)}, S_k\mathbf{x}\rangle|^2, \quad (k,\ell) \in [d] \times [2\delta - 1].$$
- *Fast Phase Retrieval from Local Correlation Measurements - Iwen, M., Viswanathan, A., Wang, Y.* analyzes phase retrieval measurements of this form, by using a lifted linear system involving a block circulant matrix $\breve{\mathbf{M}}$ and $\delta << d$ supported masks.
- Let $D = d(2\delta - 1)$. We then define the block circulant matrix $\breve{\mathbf{M}} \in \mathbb{C}^{D\times D}$ via
$$\breve{\mathbf{M}} := \begin{pmatrix} \breve{\mathbf{M}}_0 & \breve{\mathbf{M}}_1 & \dots & \breve{\mathbf{M}}_{\delta-1} & 0 & 0 & \dots & 0 \\ 0 & \breve{\mathbf{M}}_0 & \breve{\mathbf{M}}_1 & \dots & \breve{\mathbf{M}}_{\delta-1} & 0 & \dots & 0 \\ \vdots & \vdots & \vdots & \ddots & \ddots & \vdots & \vdots & \vdots \\ \breve{\mathbf{M}}_1 & \dots & \breve{\mathbf{M}}_{\delta-1} & 0 & 0 & 0 & \dots & \breve{\mathbf{M}}_0 \end{pmatrix}$$
where the matrices $\breve{\mathbf{M}}_k \in \mathbb{C}^{(2\delta-1)\times(2\delta-1)}$ are defined entry-wise by
$$(\breve{\mathbf{M}}_k)_{ij} := \begin{cases} (\breve{\mathbf{m}}_i)_k \overline{(\breve{\mathbf{m}}_i)_{j+k}}, & 0 \le j \le \delta - k \\ (\breve{\mathbf{m}}_i)_k \overline{(\breve{\mathbf{m}}_i)_{j+k-2\delta}}, & 2\delta - 1 + k \le j \le 2\delta - 2 \wedge k < \delta \\ 0, & \text{otherwise} \end{cases}$$

Condition Number Bound

- Then it is shown that $\text{vec}(\mathbf{Y}) = \check{\mathbf{M}}\mathbf{z}$ for $\mathbf{z} \in \mathbb{C}^d$ being a portion of $\text{vec}(\mathbf{x}\mathbf{x}^*)$
- Then $\mathbf{z} = \check{\mathbf{M}}^{-1} vec(\mathbf{Y})$ and we reshape $\mathbf{z}$ to recover $\widehat{\mathbf{X}}$ whose non-zero entries are estimates of the $\mathbf{x}\mathbf{x}^*$
- Angular synchronization is performed on $\widehat{\mathbf{X}}$ to recover $\mathbf{x}_{est}$
- In the paper, it is shown that exponential masks $\check{\mathbf{m}}_\ell^{(fpr)}$ defined by

$$(\check{\mathbf{m}}_\ell^{(fpr)})_n = \begin{cases} \frac{e^{-(n+1)/a}}{\sqrt[4]{2\delta-1}} \cdot e^{\frac{2\pi i n \ell}{2\delta-1}}, & n \in [\delta] \\ 0, & \text{otherwise} \end{cases}, \quad a := \max\left\{4, \frac{\delta-1}{2}\right\}$$

lead to lifted linear systems that are well-conditioned and allow for recovery guarantees.

Theorem (Theorem 4 - M. Iwen., et. al.)

For collection of masks $\check{\mathbf{m}}_\ell^{(fpr)}$, the condition number has the bound

$$\kappa := \kappa(\check{\mathbf{M}}) < \max\left\{144e^2, \frac{9e^2(\delta-1)^2}{4}\right\} \le C\delta^2, \quad C \in \mathbb{R}^+$$

Furthermore, $\check{\mathbf{M}}$ can be inverted in $\mathcal{O}(\delta \cdot d \log d)$-time.

Admissable Selection of PSF and Mask

- We would like to show there are realistic $\mathbf{p}$ and $\mathbf{m}$ with $\check{\mathbf{m}}_\ell^{(fpr)} = \overline{S_\ell \tilde{\mathbf{p}} \circ \mathbf{m}}$.
- One can show that it is impossible to choose a $\mathbf{p}$ and $\mathbf{m}$ that are independent of ℓ that accomplishes this, however we can approximate it up to a phase factor.

Lemma (Admissable Selection of PSF and Mask)

Let $\mathbf{p}, \mathbf{m} \in \mathbb{C}^d$ have entries given by

$$p_n := e^{-\frac{2\pi \mathbb{i} n^2}{2\delta-1}}, \quad \text{and} \quad m_n := \begin{cases} \frac{e^{-n+1}/a}{\sqrt[4]{2\delta-1}} \cdot e^{\frac{2\pi \mathbb{i} n^2}{2\delta-1}}, & n \in [\delta]_0 \\ 0, & \text{otherwise} \end{cases},$$

where $a := \max\left\{4, \frac{\delta-1}{2}\right\}$. Then for all $\ell \in [2\delta-1]_0$, $\breve{\mathbf{m}}_\ell^{(p,m)} = \overline{S_\ell \widetilde{\mathbf{p}} \circ \mathbf{m}}$ satisfies

$$\breve{\mathbf{m}}_\ell^{(p,m)} = e^{\frac{2\pi \mathbb{i} \ell^2}{2\delta-1}} \cdot \breve{\mathbf{m}}^{(fpr)}_{2\ell \bmod 2\delta-1},$$

- Let $\breve{\mathbf{M}}^{(\text{fpr})}$ and $\breve{\mathbf{M}}^{(p,m)}$ be our lifted linear measurement matrices obtained by $\breve{\mathbf{m}}_\ell^{(\text{fpr})}$ and $\breve{\mathbf{m}}_\ell^{(p,m)}$, respectively.
- Then $\breve{\mathbf{M}}^{(p,m)} = \mathbf{P}\breve{\mathbf{M}}^{(\text{fpr})}$, where $\mathbf{P}$ is a $D \times D$ block diagonal permutation matrix.
- Thus $\breve{\mathbf{M}}^{(p,m)}$ and $\breve{\mathbf{M}}^{(fpr)}$ have the same singular values and

$$\kappa\left(\breve{\mathbf{M}}^{(p,m)}\right) = \kappa\left(\breve{\mathbf{M}}^{(\text{fpr})}\right) \leq C\delta^2,$$

Table of Contents

Magnitude Error Bound

- For $\mathbf{x} \in \mathbb{C}^d$, we write its n^{th} entry as $x_n =: |x_n|e^{\mathbb{i}\theta_n}$
- Let $\mathbf{x}^{(\text{mag})} := (|x_0|, \ldots, |x_{d-1}|)^T, \mathbf{x}^{(\theta)} := (e^{\mathbb{i}\theta_0}, e^{\mathbb{i}\theta_1}, \ldots, e^{\mathbb{i}\theta_{d-1}})^T$
- We may then decompose $\mathbf{x}$ as $\mathbf{x} = \mathbf{x}^{(\text{mag})} \circ \mathbf{x}^{(\theta)}$

Lemma (Lemma 3 - M. Roach, et al.)

Let $\mathbf{x}_{est}$ be decomposed $\mathbf{x}_{est} = \mathbf{x}_{est}^{(mag)} \circ \mathbf{x}_{est}^{(\theta)}$. Then, we have that

$$\min_{\phi\in[0,2\pi)} \left\|\mathbf{x} - e^{\mathbb{i}\phi}\mathbf{x}_{est}\right\|_2 \leq \|\mathbf{x}\|_\infty \min_{\phi\in[0,2\pi)} \left\|\mathbf{x}_{est}^{(\theta)} - e^{\mathbb{i}\phi}\mathbf{x}^{(\theta)}\right\|_2 + \left\|\mathbf{x}^{(mag)} - \mathbf{x}_{est}^{(mag)}\right\|_2.$$

- We now utilize a restated result from *Phase Retrieval from Local Measurements: Improved Robustness via Eigenvector Based Angular Synchronization - Iwen, M., Preskitt, B., Saab, R., Viswanathan, A.*

Lemma (Lemma 3 - M. Iwen, et al.)

Let $\sigma_{\min}\left(\widetilde{\mathbf{M}}^{(p,m)}\right)$ denote the smallest singular value of the lifted measurement matrix $\widetilde{\mathbf{M}}^{(p,m)}$. Then $\left\|\mathbf{x}^{(mag)} - \mathbf{x}_{est}^{(mag)}\right\|_2 \leq C\sqrt{\dfrac{\|\mathbf{N}\|_F}{\sigma_{\min}\left(\widetilde{\mathbf{M}}^{(p,m)}\right)}}$.

Angular Error Bound

- Apply lemma to our error bound and utilize the conditioning of $\mathbf{p}, \mathbf{m}$.

Theorem (Theorem 3 - M. Roach, et al.)

Let $\mathbf{p}$ *and* $\mathbf{m}$ *be our admissible PSF, mask pair. Then, we have that*

$$\min_{\phi \in [0,2\pi)} \left\| \mathbf{x} - e^{\mathbb{i}\phi} \mathbf{x}_{est} \right\|_2 \le \|\mathbf{x}\|_\infty \min_{\phi \in [0,2\pi)} \left\| \mathbf{x}^{(\theta)}_{est} - e^{\mathbb{i}\phi} \mathbf{x}^{(\theta)} \right\|_2 + C\sqrt{d\delta \|\mathbf{N}\|_F}.$$

- In *On Recovery Guarantees for Angular Synchronization - Filbir, Krahmer, Melnyk*, authors used weighted graph approach to prove bound on $\left\| \mathbf{x}^{(\theta)}_{\text{est}} - e^{\mathbb{i}\phi} \mathbf{x}^{(\theta)} \right\|_2$.
- Let $\mathbf{X}, \widehat{\mathbf{X}}$ denote partial autocorrelation matrix corresponding to $\mathbf{x}, \mathbf{x}_{\text{est}}$
- Let $G = (V, E, \mathbf{W})$ be weighted graph, $V = [d]_0$, $E = \{(i,j) \mid i \neq j, |i-j| \bmod d < \delta\}$, and whose weight matrix $\mathbf{W}$ is defined entrywise by

$$W_{i,j} = \begin{cases} |\widehat{X}_{i,j}|^2, & 0 < |i-j| \bmod d < \delta \\ 0, & \text{otherwise} \end{cases}.$$

Graph Theoretic Approach

- Let $\mathbf{D}$ denote the weighted degree matrix, $\mathbf{L}_G := \mathbf{D} - \mathbf{W}$.
- Let τ_G denote the spectral gap (second smallest eigenvalue) of $\mathbf{L}_G$.
- Since G is connected, τ_G is strictly positive.

Theorem (Corollary 3 - F. Filbir, F. Krahmer, O. Melnyk)

Let τ_G denote the spectral gap of the associated unnormalized Laplacian $\mathbf{L}_G$. Then we have that

$$\min_{\phi\in[0,2\pi)} \left\|\mathbf{x}_{est}^{(\theta)} - e^{\mathrm{i}\phi}\mathbf{x}^{(\theta)}\right\|_2 \leq C\sqrt{1+\|\mathbf{x}_{\mathrm{est}}\|_\infty} \cdot \frac{\|\mathbf{X}-\widehat{\mathbf{X}}\|_F}{\sqrt{\tau_G}}, \quad C \in \mathbb{R}^+.$$

- We have a bound for the Frobenius norm

Lemma (Lemma 6 - M. Roach, et al.)

Let $\mathbf{p}$ and $\mathbf{m}$ be our choice of PSF and mask. Then, $\|\mathbf{X}-\widehat{\mathbf{X}}\|_F \leq C\delta\|\mathbf{N}\|_F$.

Spectral Bound of Weighted Graph

- We now seek a lower bound for our weighted spectral gap.

Theorem (General Weighted Spectral Gap Bound)

Let $G = (V, E, \mathbf{W})$ be a weighted graph and let $W_{\min}$ and W_{max} be the minimum and maximum value of any its (nonzero) weights. Then

$$\tau_G \geq \frac{2 \cdot (W_{min})^2}{W_{max}(n-1) \cdot \ diam(G_{unw})},$$

where $G_{unw} = (V, E)$ is the unweighted counterpart of G, and $diam(G_{unw})$ is the corresponding diameter.

Lemma (NFP Weighted Spectral Gap Bound)

Let $|\mathbf{x}_{est}|_{\min}$ denote the smallest magnitude of any entry in $\mathbf{x}_{est}$. For our graph G, we have that

$$\tau_G \geq \frac{|\mathbf{x}_{est}|_{\min}^4}{\|\mathbf{x}_{est}\|_\infty^2} \frac{4(\delta - 1)}{d^2}.$$

Recovery Guarantee Theorem

- We now apply the Frobenius bound and spectral gap bound to our existing error bound to obtain our main result.

Theorem (Theorem 1 - M. Roach, et al.)

Choose $\delta \in [d]_0$ such that $2\delta - 1$ divides d. One can construct a PSF $\mathbf{p} \in \mathbb{C}^d$ and a mask $\mathbf{m} \in \mathbb{C}^d$ with supp$(\mathbf{m}) \subseteq [\delta]_0$ such that we can return an estimate $\mathbf{x}_{est} \in \mathbb{C}^d$ of $\mathbf{x}$ satisfying

$$\min_{\phi \in [0,2\pi)} \|\mathbf{x}_{est} - e^{\mathrm{i}\phi}\mathbf{x}\|_2 \leq C\left(\|\mathbf{x}\|_\infty \frac{d\sqrt{\delta}\sqrt{\|\mathbf{x}_{est}\|_\infty^2 + \|\mathbf{x}_{est}\|_\infty^3}}{|\mathbf{x}_{est}|_{\min}^2} \cdot \|\mathbf{N}\|_{\mathrm{F}} + \sqrt{d\delta\|\mathbf{N}\|_{\mathrm{F}}}\right).$$

Here $C \in \mathbb{R}^+$ is an absolute constant.

Table of Contents

SNR vs. Reconstruction Error

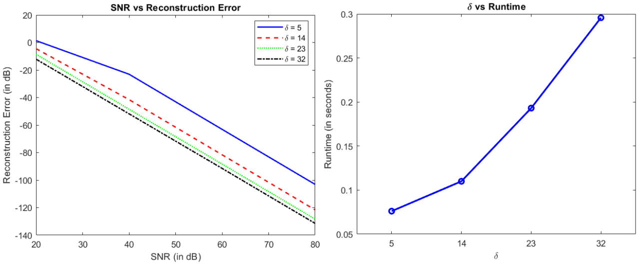

- Evaluation of algorithm with Gaussian $\mathbf{x}$ for roposed $\mathbf{p}, \mathbf{m}, d = 945$.
- Left: Reconstruction error vs SNR for various $\delta = |\mathrm{supp}(\mathbf{m})|$.
- Right: Runtime as a function of δ.
- Then the signal-to-noise ratio is given by $SNR = 10\log_{10}\left(\frac{\|\mathbf{Y}-\mathbf{N}\|_F}{\|\mathbf{N}\|_F}\right)$
- We measure the reconstruction error by $10\log_{10}\left(\frac{\min_\phi \|\mathbf{x} - e^{i\phi}\mathbf{x}_{est}\|_2^2}{\|\mathbf{x}\|_2^2}\right)$ and we plot based on varying levels of signal-to-noise ratio.

Real World Application

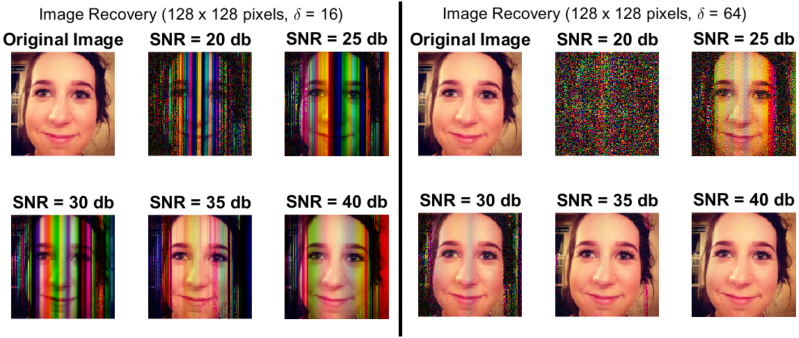

- NFP BlockPR algorithm applied to 128×128 pixel color image
- Each color channel applied separately and then combined to form final image
- $d = 128^2 = 16384$ with two delta levels applied and varying noise

Table of Contents

Far-field Ptychography

- Far-field Ptychography is when there is a large enough distance between the lens, object, and detector to obtain magnitude-square Fourier transform measurements

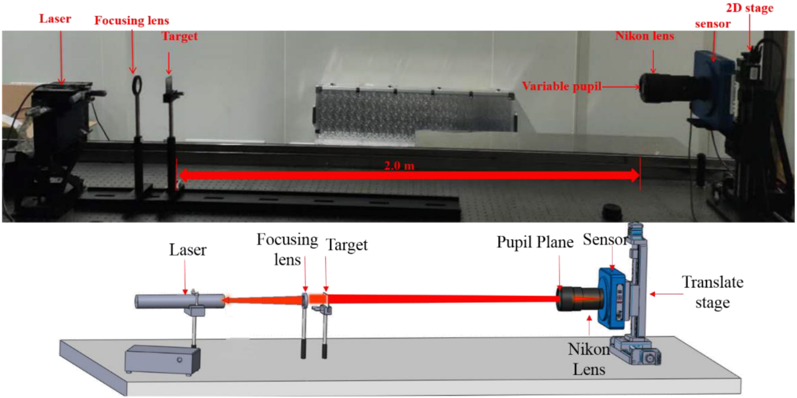

Figure: "Analysis, Simulations, and Experiments for Far-Field Fourier Ptychography Imaging Using Active Coherent Synthetic-Aperture" - Yang et al., 2022

Blind Ptychography

- Let $\mathbf{x}, \mathbf{m} \in \mathbb{C}^d$ denote the unknown object and mask, respectively.
- Suppose that we have d^2 noisy ptychographic measurements of the form

$$(\mathbf{Y})_{\ell,k} = |(\mathbf{F}(\mathbf{x} \circ S_k \mathbf{m}))_\ell|^2 + (\mathbf{N})_{\ell,k}, \quad (\ell, k) \in [d]_0 \times [d]_0.$$

- Can rewrite the measurements as

$$\left(\mathbf{Y}^T \mathbf{F}^T\right)_k = d \cdot (\mathbf{x} \circ S_k \bar{\mathbf{x}}) * (\tilde{\mathbf{m}} \circ S_{-k} \bar{\tilde{\mathbf{m}}}) + \left(\mathbf{N}^T \mathbf{F}^T\right)_k$$

- Fix k. Let $\mathbf{y}' = \left(\mathbf{Y}^T \mathbf{F}^T\right)_k, \mathbf{f} = \sqrt{d}(\tilde{\mathbf{m}} \circ S_{-k} \bar{\tilde{\mathbf{m}}}), \mathbf{g} = \sqrt{d}(\mathbf{x} \circ S_k \bar{\mathbf{x}}), \mathbf{n} = \left(\mathbf{N}^T \mathbf{F}^T\right)_k$
- This is now a noisy blind deconvolution problem i.e.

$$\mathbf{y}' = \mathbf{f} * \mathbf{g} + \mathbf{n}$$

Blind Deconvolution - Part I

- In *Rapid, Robust, and Reliable Blind Deconvolution via Nonconvex Optimization*, Strohmer et.al., demonstrated successfully recovery by utilizing reasonable assumptions
- Let $\mathbf{y} = \mathbf{f} * \mathbf{g} + \mathbf{n}$, with $\mathbf{f}, \mathbf{g}$ unknown, $\mathbf{n}$ noise
- Assume $\mathbf{f} = \begin{bmatrix} \mathbf{h} \\ \mathbf{0}_{d-K} \end{bmatrix}, \mathbf{g} = \mathbf{C}\bar{\mathbf{x}}$ for some matrix $\mathbf{C} \in \mathbb{C}^{d \times N}, N \ll d$.
- Let $\mathbf{F}_d \in \mathbb{C}^{d \times d}$ be DFT matrix, $\mathbf{B} \in \mathbb{C}^{d \times K}$ denote the first K columns of $\mathbf{F}_d$.
- Then we have that

$$\mathbf{y} = \mathbf{B}\mathbf{h} \circ \overline{\mathbf{A}\mathbf{x}} + \mathbf{e},$$

where $\mathbf{y} = \frac{1}{\sqrt{d}}\widehat{\mathbf{y}'}$, $\bar{\mathbf{A}} = \mathbf{F}_d\mathbf{C} \in \mathbb{C}^{d \times N}$, and $\mathbf{e} = \frac{1}{\sqrt{d}}\mathbf{F}_\mathbf{d}\mathbf{n}$ represents noise.

- If $(\mathbf{h}_0, \mathbf{x}_0)$ is a solution, then so is $(\alpha\mathbf{h}_0, \alpha^{-1}\mathbf{x}_0)$ for any non-zero α. Thus we assume $\|\mathbf{f}\|_2$ known.

Blind Deconvolution - Part II

- We define the matrix-valued linear operator $\mathcal{A} : \mathbb{C}^{K \times N} \longrightarrow \mathbb{C}^d$ by

$$\mathcal{A}(\mathbf{Z}) := \{\mathbf{b}_\ell^* \mathbf{Z} \mathbf{a}_\ell\}_{\ell=1}^d,$$

  where $\mathbf{b}_k$ denotes the k-th column of $\mathbf{B}^*$, and $\mathbf{a}_k$ is the k-th column of $\mathbf{A}^*$.
- Then $\mathbf{y} = \mathcal{A}(\mathbf{h}\mathbf{x}^*) + \mathbf{e}$.
- Define corresponding adjoint operator $\mathcal{A}^* : \mathbb{C}^d \longrightarrow \mathbb{C}^{K \times N}$, given by

$$\mathcal{A}^*(\mathbf{z}) := \sum_{k=1}^{d} \mathbf{z}_k \mathbf{b}_k \mathbf{a}_k^*.$$

- For any given $\mathbf{Z} \in \mathbb{C}^{K \times N}$, $\mathbb{E}(\mathcal{A}^*(\mathcal{A}(\mathbf{Z}))) = \mathbf{Z}$.
- Leading singular vectors of $\mathcal{A}^*(\mathbf{y}) \approx (\mathbf{h}, \mathbf{x})$.
- Apply gradient descent using gradients of $F(\mathbf{h}, \mathbf{x}) := \|\mathcal{A}(\mathbf{h}\mathbf{x}^*) - \mathbf{y}\|^2$

Table of Contents

Blind Ptychography Algorithm

- Let $\mathbf{y}_{(k)} = \frac{1}{\sqrt{d}} \cdot (\mathbf{F}(\overline{(\widetilde{\mathbf{FY}})^T}))_k$, $\mathbf{f}_{(k)} = \tilde{\mathbf{m}} \circ S_{-k}\overline{\tilde{\mathbf{m}}}$ (so $\|\mathbf{f}_{(k)}\|_2$ known)
- Let $\mathbf{x} = \mathbf{C}\mathbf{x}'$ for some known matrix $\mathbf{C} \in \mathbb{C}^{d \times N}, \mathbf{x}' \in \mathbb{C}^N$.

Lemma

Let $\mathbf{A} \in \mathbb{C}^{m \times n}, \mathbf{B} \in \mathbb{C}^{n \times p}, \mathbf{C} \in \mathbb{C}^{m \times q}, \mathbf{D} \in \mathbb{C}^{q \times p}$. Then we have that

$$(\mathbf{AB}) \circ (\mathbf{CD}) = (\mathbf{A} \bullet \mathbf{C})(\mathbf{B} \odot \mathbf{D}),$$

where $\circ$ is the Hadamard product, $\odot$ is the standard Khatri-Rao product, $\bullet$ is the transposed Khatri-Rao product.

- Let $\mathbf{g}_{(k)} = \mathbf{x} \circ S_k \bar{\mathbf{x}} = \mathbf{C}\mathbf{x}' \circ S_k \bar{\mathbf{C}} \bar{\mathbf{x}}'$.
- Then $\mathbf{g}_{(k)} = \mathbf{C}'_{(k)} \mathbf{x}''$ where $\mathbf{C}' \in \mathbb{C}^{d \times N^2}, \mathbf{x}'' \in \mathbb{C}^{N^2}$ are given by

$$\mathbf{C}'_{(k)} = \mathbf{C} \bullet S_k \bar{\mathbf{C}}, \; \mathbf{x}'' = \mathbf{x}' \odot \bar{\mathbf{x}}', \quad 0 \le k \le K, d - K + 1 \le k \le d.$$

- Perform $2\delta - 1$ blind deconvolutions, with $\mathbf{y}_{(k)}, \mathbf{f}_{(k)}, \mathbf{g}_{(k)}, \mathbf{C}$, as above
- We obtain $2\delta - 1$ estimates for

$$\mathbf{x}' \odot \bar{\mathbf{x}}' = vec(\mathbf{x}'(\mathbf{x}')^*)$$

.

- Use angular synchronization to solve for $2\delta - 1$ estimates $\mathbf{x}'_{est}$
- Thus solve for $2\delta - 1$ estimates

$$\mathbf{x}^i_{est} = \mathbf{C}\mathbf{x}'_{est}, \quad i \in [2\delta - 1]_0$$

.

- We use these estimates $\mathbf{x}^i_{est}$ to compute $2\delta - 1$ estimates $\mathbf{m}^j_{est}, j \in [2\delta - 1]_0$.

Computing the Mask

- From our original measurements, it can be further shown that

$$\mathbf{F}_d\left(\mathbf{Y}^T\mathbf{F}_d^T\right)_k = d \cdot \mathbf{F}_d(\mathbf{x} \circ S_k\bar{\mathbf{x}}) \circ \mathbf{F}_d(\tilde{\mathbf{m}} \circ S_{-k}\bar{\tilde{\mathbf{m}}}) + \mathbf{F}_d\left(\mathbf{N}^T\mathbf{F}_d^T\right)_k$$

- Assuming noiseless scenario, then we have that

$$\mathbf{F}_d(\tilde{\mathbf{m}} \circ S_{-k}\bar{\tilde{\mathbf{m}}}) = \frac{1}{d}\frac{\mathbf{F}_d\left(\mathbf{Y}^T\mathbf{F}_d^T\right)_k}{\mathbf{F}_d(\mathbf{x} \circ S_k\bar{\mathbf{x}})}$$

- So once we have an estimate for $\mathbf{x}$, we compute the $2\delta - 1$ pointwise divisions, then $2\delta - 1$ inverse Fourier transforms.
- These become the diagonals of a matrix which will estimate $\tilde{\mathbf{m}}\tilde{\mathbf{m}}^*$. Thus compute angular synchronization and finally a reversal.

Blind Ptychography Algorithm

- Ideally, we would want to select the estimates which generate the minimum error for each **x** and **m** i.e. find

$$\text{Min Shift}^{(x)} = \underset{\mathbf{x}^i_{est}}{\operatorname{argmin}} \|\mathbf{x} - \mathbf{x}^i_{est}\|_2^2, \quad \text{Min Shift}^{(m)} = \underset{\mathbf{m}^j_{est}}{\operatorname{argmin}} \|\mathbf{m} - \mathbf{m}^j_{est}\|_2^2$$

  for $i, j \in [2\delta - 1]_0$.
- However that implies prior knowledge of **x** and **m**.
- Instead, compute $(2\delta - 1)^2$ estimates of the Fourier measurements by

$$(\mathbf{Y}^{i,j}_{est})_{\ell,k} = |(\mathbf{F}(\mathbf{x}^i_{est} \circ S_k \mathbf{m}^j_{est}))_\ell|^2, \quad i, j \in [2\delta - 1]_0.$$

- We then compute the associated error

$$(i', j') = \underset{(i,j)}{\operatorname{argmin}} \frac{\|\mathbf{Y}^{i,j}_{est} - \mathbf{Y}\|_F^2}{\|\mathbf{Y}\|_F^2}, \quad i, j \in [2\delta - 1]_0$$

- Let $\mathbf{x}_{est} = \mathbf{x}^{i'}_{est}, \mathbf{m}_{est} = \mathbf{m}^{j'}_{est}$.

Table of Contents

SNR vs. Reconstruction Error

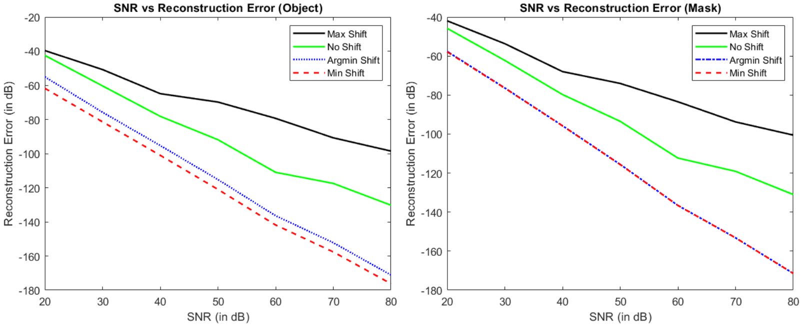

- $d = 2^6$, $K = \delta = \log_2 d$, $N = 4$, $\mathbf{C}$ complex Gaussian, 100 simulations
- Max shift refers to the maximum possible error.
- Min shift refers to the minimum possible error.
- Argmin Shift refers to the choice of object and mask chosen by our algorithm.

Table of Contents

Johnson-Lindenstrauss Lemma

- We consider real-world problems with geometric input data X and want to consider metric embeddings $X \to Y$ where $dim(Y) \ll dim(X)$
- Working with lower-dimensional embedded data typically results in efficiency gains, in terms of memory, running time, and/or other resources but reduction in accuracy

Lemma (Johnson-Lindenstrauss Lemma)

Let $\epsilon \in (0,1)$ and $X \subset \mathbb{R}^d$ be arbitrary with $|X| = n > 1$. There exists $f : X \longrightarrow \mathbb{R}^m$ with $m = O(\epsilon^{-2} \log n)$ such that $\forall x \in X, \forall \mathbf{y} \in X$

$$(1-\epsilon)\|\mathbf{x}-\mathbf{y}\|_2 \le \|f(\mathbf{x}) - f(\mathbf{y})\|_2 \le (1+\epsilon)\|\mathbf{x}-\mathbf{y}\|_2$$

- $1-\epsilon$, $1+\epsilon$, are referred to as the **distortion**, $Dist(f)$, of the embedding f
- Let X denote the set of training data in $\mathbb{R}^d$. Lemma states that distance between the training data will be preserved up to a small distortion.
- However, we want distance between the training data and any point in $\mathbb{R}^d$ (testing data) to be preserved up to a small distortion

Terminal Embedding Theorem

- Work by Elkin et.al showed that y can be taken as an arbitrary point in $\mathbb{R}^d$ with $m = \mathcal{O}(\log n)$ and distortion $\approx \sqrt{10}$.

Theorem (Theorem 1.1 - Narayanan, Nelson)

Let $\epsilon \in (0,1)$ and $X \subset \mathbb{R}^d$ be arbitrary with $|X| = n > 1$. There exists $f : X \longrightarrow \mathbb{R}^m$ with $m = \mathcal{O}(\epsilon^{-2} \log n)$ such that $\forall x \in X, \forall y \in \mathbb{R}^d$

$$(1-\epsilon)\|x-y\|_2 \leq \|f(x) - f(y)\|_2 \leq (1+\epsilon)\|x-y\|_2$$

- This embedding is called a **terminal embedding** with multiplicative factor on the right hand side referred to as the **terminal distortion**.
- If the points in X are mapped to $\mathbb{R}^m$ well, which occurs with high probability, then our final terminal embedding is guaranteed to have low terminal distortion as a map from all of $\mathbb{R}^d$ to $\mathbb{R}^m$.

Outer Extension, ϵ-Convex Hull Distortion

Definition (Outer extension)

*For $f : X \longrightarrow \mathbb{R}^m$ and $X \subset Z$, we say $g : Z \longrightarrow \mathbb{R}^{m'}$ is an **outer extension** of f if $m' \geq m$, and $g(\mathbf{x})$ being a zero-padding of $f(\mathbf{x})$, for $\mathbf{x} \in X$.*

- We define our terminal embedding by

$$f_{\text{Ext}}(\mathbf{u}) = \begin{cases} (f(\mathbf{u}), 0), & \mathbf{u} \in X \\ f^{(\mathbf{u})}(\mathbf{u}), & \mathbf{u} \in R^d \setminus X \end{cases}$$

  which is an outer extension on X, and $f^{(\mathbf{u})}$ function depending on $\mathbf{u}$
- The goal is to specify how to embed points $\mathbf{x} \in X$ and then how to embed points $\mathbf{u} \notin X$ such that we obtain low distortion.

Definition (ϵ-convex hull distortion)

*For $T \subset \mathcal{S}^{d-1}$ and $\epsilon \in (0, 1)$, we say that $\Pi \in \mathbb{R}^{m \times d}$ provides ϵ-**convex hull distortion** for T if*

$$|\,\|\Pi\mathbf{x}\|_2 - \|\mathbf{x}\|_2| < \epsilon, \quad \forall \mathbf{x} \in conv(T),$$

where $\mathcal{S}^{d-1} \subset \mathbb{R}^d$ unit sphere, $conv(T)$ convex hull of T

Construction of Terminal Embedding

Lemma (Lemma 3.2 - Narayanan, Nelson)

Let $x_1, \ldots, \mathbf{x}_n \in \mathbb{R}^d$ be distinct. Let $Y = \{\frac{\mathbf{x}_i - \mathbf{x}_j}{\|\mathbf{x}_i - \mathbf{x}_j\|_2} : i \neq j\}$. Suppose Π provides an ϵ-convex hull distortion for Y. Then $\forall \mathbf{u} \in \mathbb{R}^d$, $\exists$ outer extension f_{Ext} with $f(\mathbf{x}_i) = \Pi \mathbf{x}_i$, $f^{(\mathbf{u})}$ defined below, which provides $(1+\epsilon)$-distortion

- By choosing $\Pi \in \mathbb{R}^{m \times d}$ to have i.i.d sub-Gaussian entries, we get with high probability, a matrix providing ϵ-convex hull distortion for Y.
- To map any point $\mathbf{u}$ from $\mathbb{R}^d$ into $\mathbb{R}^{m+1}$, find $\mathbf{u}' \in \mathbb{R}^m$ such that:
- if $\mathbf{x}_{NN}$ is the point in X closest to $\mathbf{u}$, $\|\mathbf{u}'\|_2 \leq \|\mathbf{u} - \mathbf{x}_{NN}\|_2$
- $\forall i, |\langle \mathbf{u}', \Pi(\mathbf{x}_i - \mathbf{x}_{NN})\rangle - \langle \mathbf{u} - x_k, \mathbf{x}_i - \mathbf{x}_k\rangle| \leq \epsilon \|\mathbf{u} - \mathbf{x}_{NN}\|_2 \|\mathbf{x}_i - \mathbf{x}_{NN}\|_2$
- For $\mathbf{u} \in \mathbb{R}^d \setminus X$, $f^{(\mathbf{u})}(\mathbf{u}) := (\Pi \mathbf{x}_{NN} + \mathbf{u}', \sqrt{\|\mathbf{u} - \mathbf{x}_{NN}\|_2^2 - \|\mathbf{u}'\|_2^2})$

Lemma

Let Π be an ϵ-convex hull distortion for Y. Then $\mathbf{u}'$ exists for all $\mathbf{u}$, and $\mathbf{u}'$ can be found with semi-definite programming in polynomial time.

Algorithm Terminal Embedding of a Finite Set

Input: $\epsilon \in (0,1)$, $X \subset \mathbb{R}^N$, $|X| =: n$, $S \subset \mathbb{R}^N$, $|S| =: n'$, $S \cap X = \emptyset$, $m \in \mathbb{N}$ with $m < N$, a random matrix Gaussian entries, $\Phi \in \mathbb{R}^{m \times N}$, $\Pi := \frac{1}{\sqrt{m}}\Phi$

Output: A terminal embedding of X, $f \in \mathbb{R}^N \to \mathbb{R}^{m+1}$, evaluated on S

for $\mathbf{u} \in S$ **do**

1) Compute $\mathbf{x}_{NN} := \underset{\mathbf{x} \in \mathbf{X}}{\operatorname{argmin}} \|\mathbf{u} - \mathbf{x}\|_2$

2) Solve constrained minimization problem to compute $\mathbf{u}' \in \mathbb{R}^m$

$$\begin{aligned} \textit{Minimize} \quad & h_{\mathbf{u},\mathbf{x}_{NN}}(\mathbf{z}) := \|\mathbf{z}\|_2^2 + 2\langle \Pi(\mathbf{u} - \mathbf{x}_{NN}), \mathbf{z}\rangle \\ \text{subject to} \quad & \|\mathbf{z}\|_2 \le \|\mathbf{u} - \mathbf{x}_{NN}\|_2, \qquad \forall \mathbf{x} \in X \\ & |\langle \mathbf{z}, \Pi(\mathbf{x} - \mathbf{x}_{NN})\rangle - \langle \mathbf{u} - \mathbf{x}_{NN}, \mathbf{x} - \mathbf{x}_{NN}\rangle| \le \epsilon \|\mathbf{u} - \mathbf{x}_{NN}\|_2 \|\mathbf{x} - \mathbf{x}_{NN}\|_2 \end{aligned}$$

3) Compute $f : \mathbb{R}^N \to \mathbb{R}^{m+1}$ at $\mathbf{u}$ via

$$f(\mathbf{u}) := \begin{cases} (\Pi\mathbf{u}, 0), & \mathbf{u} \in X \\ \left(\Pi\mathbf{x}_{NN} + \mathbf{u}', \sqrt{\|\mathbf{u} - \mathbf{x}_{NN}\|_2^2 - \|\mathbf{u}'\|_2^2}\right), & \mathbf{u} \in S \end{cases}$$

end for

Table of Contents

Measuring Compressive Nearest Neighbor Classification Accuracy

- Let $\epsilon \in (0,1)$, labeled data set $\mathcal{D} \subset \mathbb{R}^N$: Training set $X \subset \mathcal{D}$ with $|X| =: n$, Test set $S \subset \mathcal{D}$ with $|S| =: n'$, such that $S \cap X = \emptyset$.
- Let $m \ll N$ and fix $f : \mathbb{R}^N \to \mathbb{R}^{m+1}$ such that

$$(1-\epsilon)\|\mathbf{x}-\mathbf{y}\|_2 \le \|f(\mathbf{x}) - f(\mathbf{y})\|_2 \le (1+\epsilon)\|\mathbf{x}-\mathbf{y}\|_2, \quad \mathbf{x}, \mathbf{y} \in X$$

- For $\mathbf{x} \in X, \mathbf{u} \in S$, compute $f(\mathbf{x}), f(\mathbf{u})$ using previous Algorithm
- For each $\mathbf{u} \in S$, compute $\mathbf{z} = \operatorname{argmin}_{\mathbf{y} \in X} \|f(\mathbf{u}) - f(\mathbf{y})\|_2$
- If $Label(\mathbf{u}) = Label(\mathbf{z})$, this is deemed a successful classification
- Track success rate as percentage

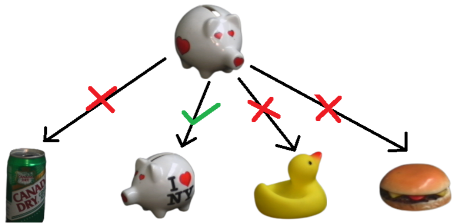

COIL-100 Dataset

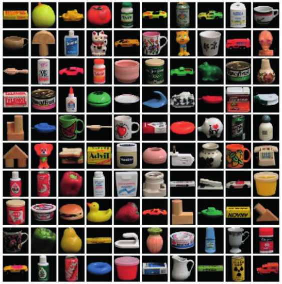

- COIL-100 dataset: 100 objects, 128×128-pixel color images of 100 objects, 72 evenly spaced rotations
- Grayscaled, vectorized, 7,200 total datapoints in $\mathbb{R}^N$ with $N = 128^2 = 16,384$
- Training data: evenly distributed, evenly rotated collection of all 100 objects

COIL-100 Classification Simulations

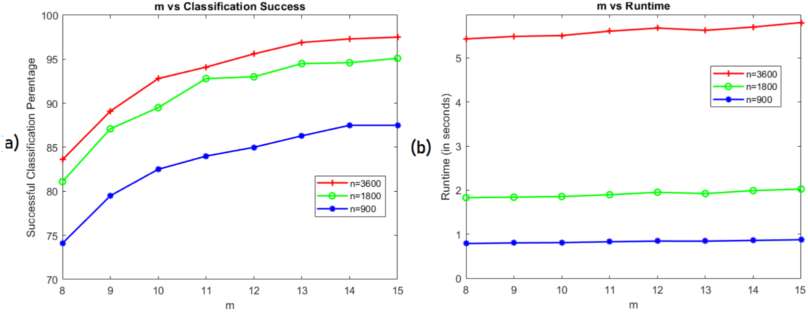

- This figure compares compressive NN classification accuracies, and the associated classification run times averaged over all $\mathbf{u} \in S$.
- Three different training data set sizes $n = |X| \in \{900, 1800, 3600\}$ were fixed as the embedding dimension $m + 1$ varied for each of the first two subfigures.

Comparison Figure

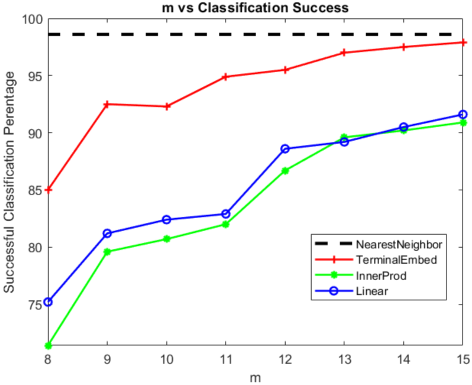

- **Nearest Neighbor**: Find the nearest neighbor in the original space
- **TerminalEmbed**: $h_{\mathbf{u},\mathbf{x}_{NN}}(\mathbf{z}) := \|\mathbf{z}\|_2^2 + 2\langle \Pi(\mathbf{u} - \mathbf{x}_{NN}), \mathbf{z}\rangle$
- **InnerProd**: $h_{\mathbf{u},\mathbf{x}_{NN}}(\mathbf{z}) := \langle \Pi(\mathbf{u} - \mathbf{x}_{NN}), \mathbf{z}\rangle$
- **Linear**: Embed into the space linearly i.e. $f(\mathbf{u}) = (\Pi\mathbf{u}, 0)$

Compressed Classification from Phaseless Measurements

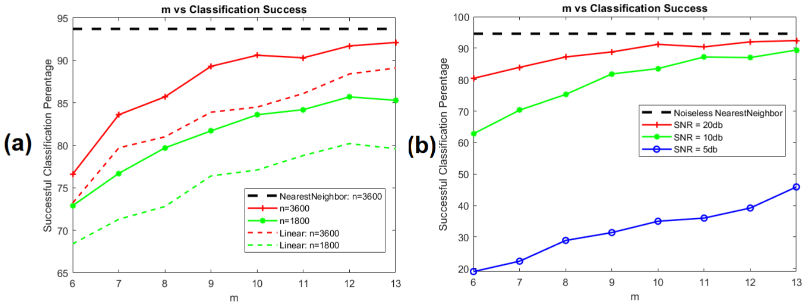

- Sub-sampled NFP measurements $|(\mathbf{p} * (S_k \mathbf{m} \circ \mathbf{x}))_\ell|^2, \ (k,\ell) \in [d]_0 \times [1]_0$
- $\mathbf{x}$ = vectorized, grayscaled, COIL-100 images
- Left: Comparing NearestNeighbor, TerminalEmbed, & Linear
- Right: Additive noise applied to testing data i.e. $\mathbf{u} \to \mathbf{u} + \mathbf{n}$

Table of Contents

Reach

Definition

For a subset $S \subset \mathbb{R}^N$ of Euclidean space, the **reach** τ_S is

$$\tau_S := \sup\left\{t \geq 0 \,\middle|\, \forall \mathbf{x} \in \mathbb{R}^n \text{s.t.} d(\mathbf{x}, S) < t, \mathbf{x} \text{ has a unique closest point in } S\right\}.$$

- All points within distance τ_S of S have unique nearest Euclidean neighbors on S
- $\tau_S = \infty \Leftrightarrow S \subseteq \mathbb{R}^N$ is closed and convex.
- Larger $\tau_S \Rightarrow S$ simple (flatter, non-self-intersecting, etc.)

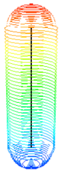

reach(line segment) $= \infty$

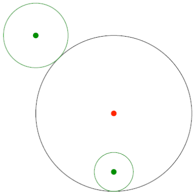

reach(sphere) $=$ radius of sphere

Gaussian Width, Unit Secants, Volume

Definition

The **Gaussian width** of a set $T \subset \mathbb{R}^N$ is $w(T) := \mathbb{E}\sup_{\mathbf{x}\in T}\langle \mathbf{g}, \mathbf{x}\rangle$, where $\mathbf{g}$ is a random vector with N i.i.d. mean 0 and variance 1 Gaussian entries.

- Gaussian width can replace cardinality as measure of set complexity.
- If T is unit ℓ_2 ball in a N-dimensional subspace, then $w(T) \approx \sqrt{N}$

Definition

We define the **unit secants of** $T \subset \mathbb{R}^N$ to be

$$S_T := \overline{U\left((T-T)\setminus\{\mathbf{0}\}\right)} = \overline{\left\{\frac{\mathbf{x}-\mathbf{y}}{\|\mathbf{x}-\mathbf{y}\|_2} \,\middle|\, \mathbf{x},\mathbf{y}\in T,\ \mathbf{x}\neq\mathbf{y}\right\}}.$$

- Let $\mathcal{M} \hookrightarrow \mathbb{R}^N$ be a compact d-dimensional submanifold of $\mathbb{R}^N$ with boundary $\partial\mathcal{M}$, finite reach $\tau_{\mathcal{M}}$, and volume $V_{\mathcal{M}}$.
- τ_i = reach of i^{th} connected component of $\partial\mathcal{M}$ as submanifold of $\mathbb{R}^N$.
- Set $\tau := \min_i\{\tau_{\mathcal{M}}, \tau_i\}$, let $V_{\partial\mathcal{M}} = Vol(\partial\mathcal{M})$, and $\omega_d = Vol(B_d(1))$.

Theorem (The Main Result)

Let $d \geq 2$. Define $\alpha_{\mathcal{M}} := \frac{V_{\mathcal{M}}}{\omega_d}\left(\frac{41}{\tau}\right)^d + \frac{V_{\partial\mathcal{M}}}{\omega_{d-1}}\left(\frac{81}{\tau}\right)^{d-1}$. Fix $\epsilon \in (0,1)$ and define $\beta_{\mathcal{M}} := \left(\alpha_{\mathcal{M}}^2 + 3^d \alpha_{\mathcal{M}}\right)$. Then, there exists a map $f : \mathbb{R}^N \to \mathbb{C}^m$ with $m \leq c\left(\ln\left(\beta_{\mathcal{M}}\right) + 4d\right)/\epsilon^2$ that satisfies

$$(1-\epsilon)\left\|\mathbf{x}-\mathbf{y}\right\|_2^2 \leq \left\|f(\mathbf{x}) - f(\mathbf{y})\right\|_2^2 \leq (1+\epsilon)\left\|\mathbf{x}-\mathbf{y}\right\|_2^2$$

for all $\mathbf{x} \in \mathcal{M}$ and $\mathbf{y} \in \mathbb{R}^N$. Here $c \in \mathbb{R}^+$ is an absolute constant.

The following theorem bounds the Gaussian width of a smooth submanifold of $\mathbb{R}^N$ in terms of its dimension, reach, and volume.

Theorem (Theorem 2.1 - Iwen, Roach)

Let $d \geq 2$. Define $\alpha_{\mathcal{M}} := \frac{V_{\mathcal{M}}}{\omega_d}\left(\frac{41}{\tau}\right)^d + \frac{V_{\partial\mathcal{M}}}{\omega_{d-1}}\left(\frac{81}{\tau}\right)^{d-1}$, $\beta_{\mathcal{M}} := \left(\alpha_{\mathcal{M}}^2 + 3^d \alpha_{\mathcal{M}}\right)$. Then we have that

$$w\left(S_{\mathcal{M}}\right) \leq 8\sqrt{2}\sqrt{\ln\left(\beta_{\mathcal{M}}\right) + 4d}.$$

Proof of Main Result

- $\Phi \in \mathbb{C}^{m \times N}$ with independent, isotropic, sub-Gaussian rows provides ϵ-convex hull distortion for $S_{\mathcal{M}}$.
- This forms the basis for our outer bi-Lipschitz extension f

Theorem (Theorem 3.2 - Iwen, Roach)

Let $\mathcal{M} \subset \mathbb{R}^N$ and $\epsilon \in (0,1)$. There exists a map $f : \mathbb{R}^N \to \mathbb{C}^m$ with $m \leq c\left(\frac{w(S_{\mathcal{M}})}{\epsilon}\right)^2$ that satisfies

$$(1-\epsilon)\,\|\mathbf{x}-\mathbf{y}\|_2^2 \leq \|f(\mathbf{x}) - f(\mathbf{y})\|_2^2 \leq (1+\epsilon)\,\|\mathbf{x}-\mathbf{y}\|_2^2$$

for all $\mathbf{x} \in \mathcal{M}$ and $\mathbf{y} \in \mathbb{R}^N$, where $c \in \mathbb{R}^+$ is an absolute constant.

Proof of Main Result.

Theorem 3.2 proves that there exists a terminal embedding $f : \mathbb{R}^N \to \mathbb{C}^m$ with $m \leq c\left(\frac{w(S_{\mathcal{M}})}{\epsilon}\right)^2$. Theorem 2.1 bounds $w(S_{\mathcal{M}})$. Apply both theorems to complete proof. $\square$

References - Near-field Ptychography

- Iwen, M., Perlmutter, M., Roach, M.P., **Toward Fast and Provably Accurate Near-field Ptychographic Phase Retrieval**, *Sampling Theory,Signal Processing, and Data Analysis, Vol 21*
- Filbir, F., Krahmer, F., Melnyk, O.
  On Recovery Guarantees for Angular Synchronization
  Fourier Anal Appl 27, 31, 2021
- Iwen, M., Preskitt, B., Saab, R., Viswanathan, A.
  Phase Retrieval from Local Measurements: Improved Robustness via Eigenvector Based Angular Synchronization
  Applied and Computational Harmonic Analysis, Vol. 48, Issue 1, pp. 415-444, 2020,
- Iwen, M., Viswanathan, A., Wang, Y.
  Fast Phase Retrieval from Local Correlation Measurements
  SIAM J. Imaging Sciences, Vol. 9, No. 4, pp. 1655 - 1688
- Zhang, H., Jiang, S., Liao, J., Deng, J., Liu, J., Zhang, Y., Zheng, G.
  Near-field Fourier Ptychography: Super-Resolution Phase Retrieval via Speckle Illumination
  Opt. Express277498-512, 2019

References - Blind Ptychography via Blind Deconvolution

- Perlmutter, M., Merhi, S., Viswanathan, A., Iwen, M.,
  Inverting Spectrogram Measurements via Aliased Wigner Distribution Deconvolution and Angular Synchronization
  https://arxiv.org/abs/1907.10773
- Iwen, M., Merhi, S., Perlmutter, M.,
  Lower Lipschitz Bounds for Phase Retrieval from Locally Supported Measurements
  https://arxiv.org/abs/1806.08262
- Merhi, S.,
  PhD Thesis
  https://d.lib.msu.edu/etd/47915/datastream/OBJ/View/
- Li, X., Ling, S., Strohmer, T., Wei, K.,
  Rapid, Robust, and Reliable Blind Deconvolution via Nonconvex Optimization
  https://arxiv.org/abs/1606.04933
- Ahmed, A., Recht, B., Romberg, J.,
  Blind Deconvolution using Convex Programming
  https://arxiv.org/abs/1211.5608

References - Terminal Manifold Embeddings

- Narayanan, S., Nelson, J.,
  Optimal terminal dimensionality reduction in Euclidean space
  https://arxiv.org/abs/1810.09250
- Iwen, M., Tavakoli, A., Schmidt, B.,
  Lower Bounds on the Low-Distortion Embedding Dimension of Submanifolds of $\mathbb{R}^n$
  https://arxiv.org/abs/2105.13512
- Iwen, M., Tavakoli, A., Schmidt, B.,
  On Fast Johnson-Lindenstrauss Embeddings of Compact Submanifolds of $\mathbb{R}^N$ with Boundary
  https://arxiv.org/abs/2110.04193
- Iwen, M., Roach, M.P.,
  On Outer Bi-Lipschitz Extensions of Linear Johnson-Lindenstrauss Embeddings of Low-Dimensional Submanifolds of $\mathbb{R}^N$
  https://arxiv.org/abs/2206.03376

Questions

- Code/slides available at *https://github.com/MarkPhilipRoach*

Any questions?

Angular Synchronization

Example (Angular Synchronization)

Let $d = 4, \delta = 2$. Then $\widehat{\mathbf{X}}$ is given by

$$\widehat{\mathbf{X}} = \begin{pmatrix} |(\mathbf{x}_{est})_0|^2 & (\mathbf{x}_{est})_0\overline{(\mathbf{x}_{est})_1} & 0 & (\mathbf{x}_{est})_0\overline{(\mathbf{x}_{est})_3} \\ (\mathbf{x}_{est})_1\overline{(\mathbf{x}_{est})_0} & |(\mathbf{x}_{est})_1|^2 & (\mathbf{x}_{est})_1\overline{(\mathbf{x}_{est})_2} & 0 \\ 0 & (\mathbf{x}_{est})_2\overline{(\mathbf{x}_{est})_1} & |(\mathbf{x}_{est})_2|^2 & (\mathbf{x}_{est})_2\overline{(\mathbf{x}_{est})_3} \\ (\mathbf{x}_{est})_3\overline{(\mathbf{x}_{est})_0} & 0 & (\mathbf{x}_{est})_3\overline{(\mathbf{x}_{est})_2} & |(\mathbf{x}_{est})_3|^2 \end{pmatrix}.$$

One may verify that the lead eigenvector is $\mathbf{u} = (e^{\mathbb{i}\theta_0} \; e^{i\theta_1} \; e^{i\theta_2} \; e^{\mathbb{i}\theta_3})^T$ and therefore

$$\mathbf{x}_{est} = \sqrt{diag(\widehat{\mathbf{X}})} \circ \mathbf{u} = (|(\mathbf{x}_{est})_0|e^{\mathbb{i}\theta_0} \; |(\mathbf{x}_{est})_1|e^{\mathbb{i}\theta_1} \; |(\mathbf{x}_{est})_2|e^{\mathbb{i}\theta_2} \; |(\mathbf{x}_{est})_3|e^{\mathbb{i}\theta_3})^T.$$

- Want to be able to assume **p** is a low pass filter and be able to take fewer shifts.
- In *"Phase Retrieval via Wirtinger Flow: Theory and Algorithms - Candes, Li, Soltanolkotabi"*, quadratic equations of the form $y_n = |\langle \mathbf{m}_\ell, \mathbf{x} \rangle|^2, \; n = 1, 2, \ldots, N$ are solved by applying a gradient descent like algorithm

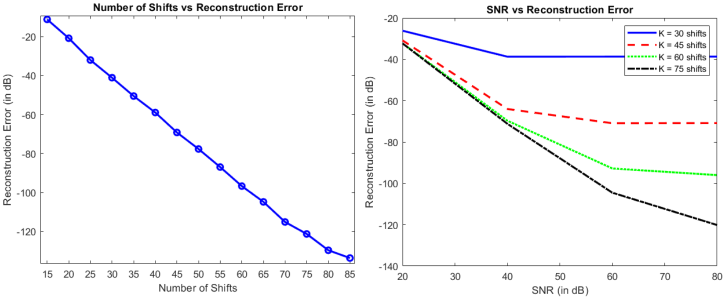

Plotting reconstruction error with $d = 102$, $\mathcal{L} = [d]_0$, and number of iterations $T = 2000$.
Left: Reconstruction error vs the number of total shifts K for fixed SNR = 80.
Right: Reconstruction error vs SNR for various numbers of shifts K.

Comparison Between Algorithms

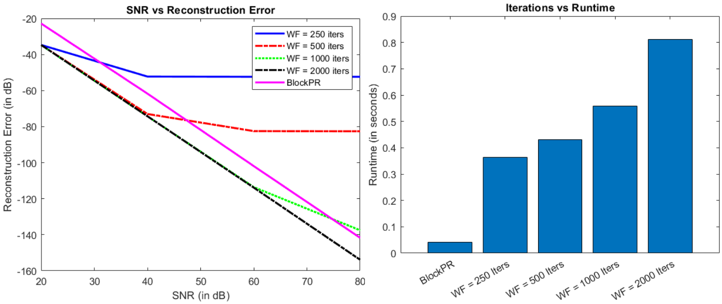

- A comparison of BlockPR and Wirtinger Flow algorithms for the proposed PSF and mask with $\delta = 26$ and $d = 102$.
- Left: Reconstruction error vs SNR for various numbers of Wirtinger Flow iterations.
- Right: The corresponding average runtimes.

Frequency of Indices

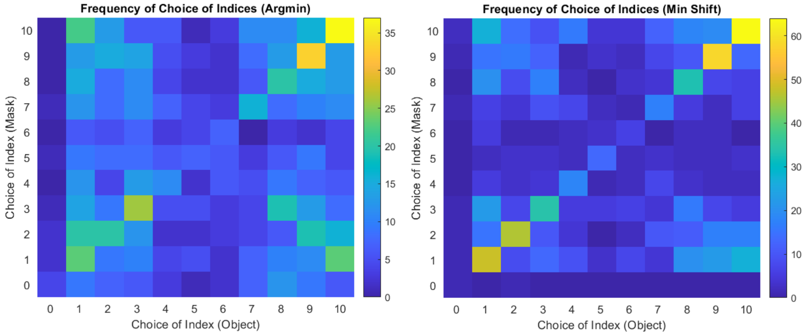

- $d = 2^6, \delta = 6, N = 4$, **C** complex Gaussian, 1000 simulations
- Left: Frequency of indices being chosen to compute (Argmin Shift$^{(x)}$, Argmin Shift$^{(m)}$)
- Right: Frequency of indices being chosen to compute (Min Shift$^{(x)}$, Min Shift$^{(m)}$).

MNIST

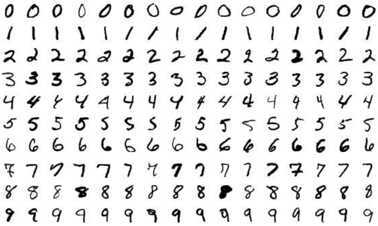

- The MNIST data set consists of 60,000 training images of 28×28-pixel grayscale hand-written images of the digits 0 through 9.
- Thus, MNIST has 10 labels to correctly classify between, and $N = 28^2 = 784$.
- For all experiments involving the MNIST dataset, $n/10$ digits of each type are selected uniformly at random to form the training set X, for a total of n vectorized training images in $\mathbb{R}^{784}$.
- Then, 100 digits of each type are randomly selected from those not used for training in order to form the test set S, leading to a total of $n' = 1000$ vectorized test images in $\mathbb{R}^{784}$.

MNIST Classification Simulations

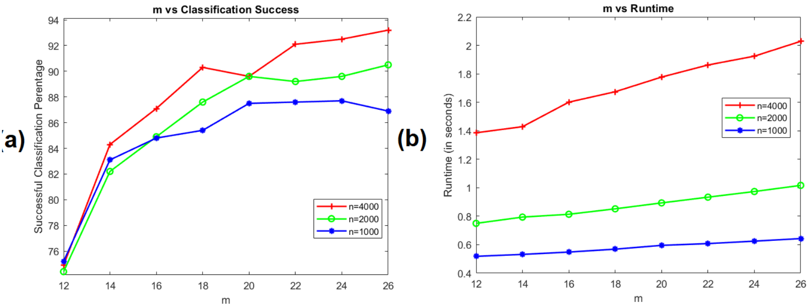

- This figure compares compressive NN classification accuracies, and the associated classification run times averaged over all $\mathbf{u} \in S$.
- Three different training data set sizes $n = |X| \in \{1000, 2000, 4000\}$ were fixed as the embedding dimension $m + 1$ varied for each of the first two subfigures.
- Recall that the test set size is always fixed to $n' = 1000$.

Non-linearity

Lemma

The terminal embedding is non-linear

Proof.

- Let $X \subset \mathbb{R}^d$ be arbitrary
- Suppose for contradiction that $f : X \longrightarrow \mathbb{R}^m, d > m$ is a linear embedding with constant terminal distortion.
- By the Rank-Nullity theorem, $dim(ker(f)) \geq d - m \geq 1$.
- This means $\exists y \in ker(f) \setminus \{0\}$
- Let $x \in X$ be arbitrary. Since f is a linear embedding and $x - y \in \mathbb{R}^d$

$$||x - (x - y)||_2 \leq ||f(x) - f(x - y)||_2$$
$$\Rightarrow 0 < ||y||_2 \leq ||f(x) - f(x) + f(y)||_2 = ||f(y)||_2 = 0$$

- Thus we have arrived at a contradiction

□

Distortion Simulations

Theorem (Theorem 1.1 - Narayanan, Nelson)

Let $\epsilon \in (0,1)$ and $X \subset \mathbb{R}^d$ be arbitrary with $|X| = n > 1$. There exists $f : X \longrightarrow \mathbb{R}^m$ with $m = \mathcal{O}(\epsilon^{-2} \log n)$ such that $\forall x \in X, \forall y \in \mathbb{R}^d$

$$(1-\epsilon)\|x-y\|_2 \leq \|f(x)-f(y)\|_2 \leq (1+\epsilon)\|x-y\|_2$$

Definition

To compute the effective distortions of a given (terminal) embedding of training data X, $f : \mathbb{R}^N \to \mathbb{R}^{m+1}$, over all available test and train data $X \cup S$ we use

$$\mathrm{MaxDist}_f = \max_{\mathbf{x}\in X} \max_{\mathbf{u}\in S\cup X\setminus\{\mathbf{x}\}} \frac{\|f(\mathbf{u})-f(\mathbf{x})\|_2}{\|\mathbf{u}-\mathbf{x}\|_2},$$

$$\mathrm{MinDist}_f = \min_{\mathbf{x}\in X} \min_{\mathbf{u}\in S\cup X\setminus\{\mathbf{x}\}} \frac{\|f(\mathbf{u})-f(\mathbf{x})\|_2}{\|\mathbf{u}-\mathbf{x}\|_2}.$$

Distortion Simulations

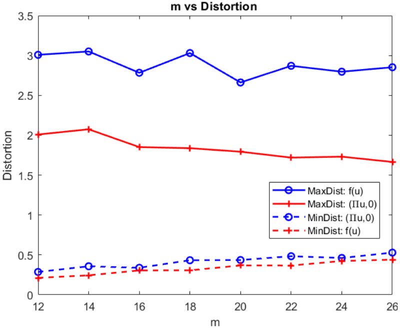

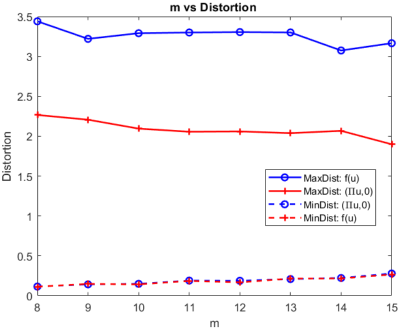

- Left figure compares MaxDist_f and MinDist_f for the nonlinear f versus its component linear embedding $\mathbf{u} \mapsto (\Pi\mathbf{u}, 0)$ as m varies for a fixed embedded training set size of $n = 4000$.
- Right figure compares MaxDist_f and MinDist_f for COIL-100 dataset, for the nonlinear f versus its component linear embedding $\mathbf{u} \mapsto (\Pi\mathbf{u}, 0)$ as m varies for a fixed embedded training set size of $n = 3600$.

Algorithm Measuring Compressive Nearest Neighbor Classification Accuracy

Input: $\epsilon \in (0, 1)$, A labeled data set $\mathcal{D} \subset \mathbb{R}^N$ split into two disjoint subsets: A training set $X \subset \mathcal{D}$ with $|X| =: n$, and a test set $S \subset \mathcal{D}$ with $|S| =: n'$, such that $S \cap X = \emptyset$. A compressive dimension $m < N$.

Output: Successful Nearest Neighbor Classification Percentage for Data Embedded in $\mathbb{R}^{m+1}$

Fix $f : \mathbb{R}^N \to \mathbb{R}^{m+1}$, an embedding of the training data $X \subset \mathbb{R}^N$ into $\mathbb{R}^{m+1}$ satisfying

$$(1 - \epsilon)\|\mathbf{x} - \mathbf{y}\|_2 \leq \|f(\mathbf{x}) - f(\mathbf{y})\|_2 \leq (1 + \epsilon)\|\mathbf{x} - \mathbf{y}\|_2$$

for all $\mathbf{x}, \mathbf{y} \in X$. [Note: this can either be a JL-embedding of X, or a stronger terminal embedding of X.]

% *Embed the training data into* $\mathbb{R}^{m+1}$.

for $\mathbf{x} \in X$ **do**

  Compute $f(\mathbf{x})$ using previous Algorithm

end for

Algorithm Measuring Compressive Nearest Neighbor Classification Accuracy

% *Classify the test data using its embedded distance in* $\mathbb{R}^{m+1}$.
$p = 0$
for $\mathbf{u} \in S$ **do**
  Compute $f(\mathbf{u})$ using, e.g., Algorithm 1
  Compute $\mathbf{x} = \operatorname{argmin}_{\mathbf{y} \in X} \|f(\mathbf{u}) - f(\mathbf{y})\|_2$
  if $Label(\mathbf{u}) = Label(\mathbf{x})$ **then**
    $p = p + 1$
  end if
end for

Output the Successful Classification Percentage = $\frac{p}{n'} \times 100\%$

Comparison Figures

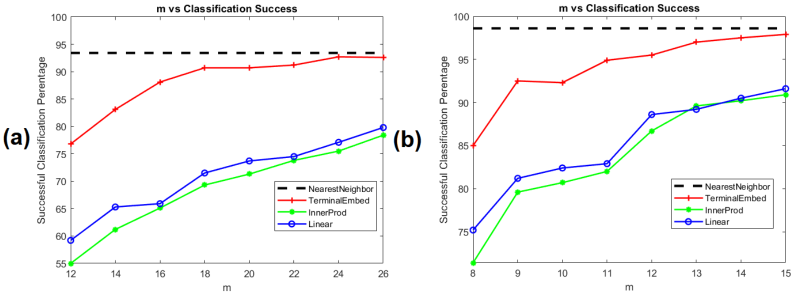

- Left: MNIST, Right: COIL-100
- **Nearest Neighbor**: Find the nearest neighbor in the original space
- **TerminalEmbed**: $h_{\mathbf{u},\mathbf{x}_{NN}}(\mathbf{z}) := \|\mathbf{z}\|_2^2 + 2\langle \Pi(\mathbf{u} - \mathbf{x}_{NN}), \mathbf{z}\rangle$
- **InnerProd**: $h_{\mathbf{u},\mathbf{x}_{NN}}(\mathbf{z}) := \langle \Pi(\mathbf{u} - \mathbf{x}_{NN}), \mathbf{z}\rangle$
- **Linear**: Embed into the space linearly i.e. $f(\mathbf{u}) = (\Pi\mathbf{u}, 0)$

COIL-100

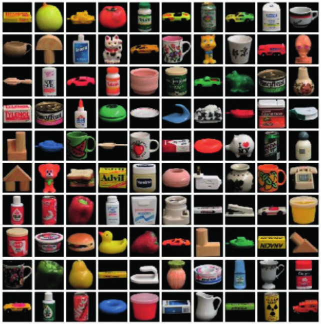

- The COIL-100 data set is a collection of 128×128-pixel color images of 100 objects, each photographed 72 times where the object has been rotated by 5 degrees each time to get a complete rotation.
- However, only the green color channel of each image is used herein for simplicity. Thus, herein COIL-100 consists of $7,200$ total vectorized images in $\mathbb{R}^N$ with $N = 128^2 = 16,384$, where each image has one of 100 different labels (72 images per label).

COIL-100

- For all experiments involving this COIL-100 data set, $n/100$ training images are down sampled from each of the 100 objects' rotational image sequences.
- Thus, the training sets each contain $n/100$ vectorized images of each object, each photographed at rotations of $\approx 36000/n$ degrees (rounded to multiples of 5). The resulting training data sets therefore all consist of n vectorized images in $\mathbb{R}^{16,384}$.
- After forming each training set, 10 images of each type are then randomly selected from those not used for training in order to form the test set S, leading to a total of $n' = 1000$ vectorized test images in $\mathbb{R}^{16,384}$ per experiment.

Gaussian Width of the Unit Secants

The following theorem bounds the Gaussian width of a smooth submanifold of $\mathbb{R}^N$ in terms of its dimension, reach, and volume.

Theorem (Theorem 2.1 - Iwen, Roach)

Let $\mathcal{M} \hookrightarrow \mathbb{R}^N$ be a compact d-dimensional submanifold of $\mathbb{R}^N$ with boundary $\partial\mathcal{M}$, finite reach $\tau_{\mathcal{M}}$, and volume $V_{\mathcal{M}}$. Enumerate the connected components of $\partial\mathcal{M}$ and let τ_i be the reach of the i^{th} connected component of $\partial\mathcal{M}$ as a submanifold of $\mathbb{R}^N$. Set $\tau := \min_i\{\tau_{\mathcal{M}}, \tau_i\}$, let $V_{\partial\mathcal{M}}$ be the volume of $\partial\mathcal{M}$, and denote the volume of the d-dimensional Euclidean ball of radius 1 by ω_d. Next,

1. *if $d = 1$, define $\alpha_{\mathcal{M}} := \frac{20 V_{\mathcal{M}}}{\tau} + V_{\partial\mathcal{M}}$, else*
2. *if $d \geq 2$, define $\alpha_{\mathcal{M}} := \frac{V_{\mathcal{M}}}{\omega_d}\left(\frac{41}{\tau}\right)^d + \frac{V_{\partial\mathcal{M}}}{\omega_{d-1}}\left(\frac{81}{\tau}\right)^{d-1}$.*

Finally, define $\beta_{\mathcal{M}} := \left(\alpha_{\mathcal{M}}^2 + 3^d \alpha_{\mathcal{M}}\right)$. Then, the Gaussian width of $\overline{U\left((\mathcal{M} - \mathcal{M}) \setminus \{\mathbf{0}\}\right)}$ satisfies

$$w\left(S_{\mathcal{M}}\right) = w\left(\overline{U\left((\mathcal{M} - \mathcal{M}) \setminus \{\mathbf{0}\}\right)}\right) \leq 8\sqrt{2}\sqrt{\ln\left(\beta_{\mathcal{M}}\right) + 4d}.$$

Main Result

Theorem (The Main Result)

Let $\mathcal{M} \hookrightarrow \mathbb{R}^N$ be a compact d-dimensional submanifold of $\mathbb{R}^N$ with boundary $\partial\mathcal{M}$, finite reach $\tau_{\mathcal{M}}$, and volume $V_{\mathcal{M}}$. Enumerate the connected components of $\partial\mathcal{M}$ and let τ_i be the reach of the i^{th} connected component of $\partial\mathcal{M}$ as a submanifold of $\mathbb{R}^N$. Set $\tau := \min_i\{\tau_{\mathcal{M}}, \tau_i\}$, let $V_{\partial\mathcal{M}}$ be the volume of $\partial\mathcal{M}$, and denote the volume of the d-dimensional Euclidean ball of radius 1 by ω_d. Next,

1. *if $d = 1$, define $\alpha_{\mathcal{M}} := \frac{20V_{\mathcal{M}}}{\tau} + V_{\partial\mathcal{M}}$, else*
2. *if $d \geq 2$, define $\alpha_{\mathcal{M}} := \frac{V_{\mathcal{M}}}{\omega_d}\left(\frac{41}{\tau}\right)^d + \frac{V_{\partial\mathcal{M}}}{\omega_{d-1}}\left(\frac{81}{\tau}\right)^{d-1}$.*

Finally, fix $\epsilon \in (0,1)$ and define $\beta_{\mathcal{M}} := \left(\alpha_{\mathcal{M}}^2 + 3^d\alpha_{\mathcal{M}}\right)$. Then, there exists a map $f : \mathbb{R}^N \to \mathbb{C}^m$ with $m \leq c\left(\ln\left(\beta_{\mathcal{M}}\right) + 4d\right)/\epsilon^2$ that satisfies

$$\left|\|f(\mathbf{x}) - f(\mathbf{y})\|_2^2 - \|\mathbf{x} - \mathbf{y}\|_2^2\right| \leq \epsilon\,\|\mathbf{x} - \mathbf{y}\|_2^2$$

for all $\mathbf{x} \in \mathcal{M}$ and $\mathbf{y} \in \mathbb{R}^N$. Here $c \in \mathbb{R}^+$ is an absolute constant.

Theorem 3.1, 3.2

Theorem (Theorem 3.1 - Iwen, Roach)

Let $\mathcal{M} \subset \mathbb{R}^N$, $\epsilon \in (0,1)$, and suppose that $\Phi \in \mathbb{C}^{m \times N}$ is an $\left(\frac{\epsilon^2}{2304}\right)$-JL map of $S_{\mathcal{M}} + S_{\mathcal{M}}$ into $\mathbb{C}^m$. Then, there exists an outer bi-Lipschitz extension of $\Phi : \mathcal{M} \to \mathbb{C}^m$, $f : \mathbb{R}^N \to \mathbb{C}^{m+1}$, with the property that

$$\left| \|f(\mathbf{x}) - f(\mathbf{y})\|_2^2 - \|\mathbf{x} - \mathbf{y}\|_2^2 \right| \leq \epsilon \|\mathbf{x} - \mathbf{y}\|_2^2$$

holds for all $\mathbf{x} \in \mathcal{M}$ and $\mathbf{y} \in \mathbb{R}^N$.

Theorem (Theorem 3.2 - Iwen, Roach)

Let $\mathcal{M} \subset \mathbb{R}^N$ and $\epsilon \in (0,1)$. There exists a map $f : \mathbb{R}^N \to \mathbb{C}^m$ with $m \leq c\left(\frac{w(S_{\mathcal{M}})}{\epsilon}\right)^2$ that satisfies

$$\left| \|f(\mathbf{x}) - f(\mathbf{y})\|_2^2 - \|\mathbf{x} - \mathbf{y}\|_2^2 \right| \leq \epsilon \|\mathbf{x} - \mathbf{y}\|_2^2$$

for all $\mathbf{x} \in \mathcal{M}$ and $\mathbf{y} \in \mathbb{R}^N$, where $c \in \mathbb{R}^+$ is an absolute constant.

Proof of Theorem 3.1

Theorem (Theorem 3.4 - Iwen, Roach)

Let $\mathcal{M} \subset \mathbb{R}^N$, $\epsilon \in (0,1)$, and suppose that $\Phi \in \mathbb{C}^{m \times N}$ is an $\left(\frac{\epsilon^2}{4}\right)$-JL map of $S_{\mathcal{M}} + S_{\mathcal{M}}$ into $\mathbb{C}^m$. Then, Φ will also provide ϵ-convex hull distortion for $S_{\mathcal{M}}$.

Lemma (Lemma 3.4 - Iwen, Roach)

Let $\mathcal{M} \subset \mathbb{R}^N$ be non-empty, $\epsilon \in (0,1)$, and suppose that $\Phi \in \mathbb{C}^{m \times N}$ provides ϵ-convex hull distortion for $S_{\mathcal{M}}$. Then, there exists an outer bi-Lipschitz extension of Φ, $f : \mathbb{R}^N \to \mathbb{C}^{m+1}$, with the property that

$$\left| \|f(\mathbf{x}) - f(\mathbf{y})\|_2^2 - \|\mathbf{x} - \mathbf{y}\|_2^2 \right| \leq 24\epsilon \|\mathbf{x} - \mathbf{y}\|_2^2$$

holds for all $\mathbf{x} \in \mathcal{M}$ and $\mathbf{y} \in \mathbb{R}^N$.

Proof of Theorem 3.1.

Apply Theorem 3.4 with $\epsilon \leftarrow \epsilon/24$ in order obtain $\epsilon/24$-convex hull distortion for $S_{\mathcal{M}}$ via Φ. Then, apply Lemma 3.4. $\square$

Proof of Theorem 3.2

Corollary (Corollary 3.1 - Iwen, Roach)

Let $\mathcal{M} \subset \mathbb{R}^N$, $\epsilon, p \in (0,1)$, and $\Phi \in \mathbb{R}^{m \times N}$ be an $m \times N$ matrix whose rows are independent, isotropic, and sub-Gaussian random vectors in $\mathbb{R}^N$. Furthermore, suppose that

$$m \geq \frac{c'}{\epsilon^2} \left(w\left(S_{\mathcal{M}}\right) + \sqrt{\ln(2/p)} \right)^2,$$

where c' is a constant depending only on the distribution of the rows of Φ. Then, with probability at least $1 - p$, $\frac{1}{\sqrt{m}} \Phi$ will be an ϵ-JL embedding of $\mathcal{M}$ into $\mathbb{R}^m$ and provide ϵ-convex hull distortion for $S_{\mathcal{M}}$.

Proof of Theorem 3.2.

- Apply Corollary 3.1 with $p = 1/2$ to demonstrate that a $\left\lceil \frac{c''}{\epsilon^2} \left(w(S_{\mathcal{M}}) + \sqrt{\ln(4)} \right)^2 \right\rceil \times N$ matrix with i.i.d. standard normal random entries can provide $(\epsilon/24)$-convex hull distortion for $S_{\mathcal{M}}$, where c'' is an absolute constant.
- Apply Lemma 3.4 to finish the proof.

$\square$

Main Result

Theorem (The Main Result)

Let $d \geq 2$. Define $\alpha_{\mathcal{M}} := \frac{V_{\mathcal{M}}}{\omega_d}\left(\frac{41}{\tau}\right)^d + \frac{V_{\partial\mathcal{M}}}{\omega_{d-1}}\left(\frac{81}{\tau}\right)^{d-1}$. Fix $\epsilon \in (0,1)$ and define $\beta_{\mathcal{M}} := \left(\alpha_{\mathcal{M}}^2 + 3^d\alpha_{\mathcal{M}}\right)$. Then, there exists a map $f : \mathbb{R}^N \to \mathbb{C}^m$ with $m \leq c\left(\ln\left(\beta_{\mathcal{M}}\right) + 4d\right)/\epsilon^2$ that satisfies

$$\left|\|f(\mathbf{x}) - f(\mathbf{y})\|_2^2 - \|\mathbf{x} - \mathbf{y}\|_2^2\right| \leq \epsilon\,\|\mathbf{x} - \mathbf{y}\|_2^2$$

for all $\mathbf{x} \in \mathcal{M}$ and $\mathbf{y} \in \mathbb{R}^N$. Here $c \in \mathbb{R}^+$ is an absolute constant.

Proof of Main Result.

- Theorem 3.2 proves that there exists a map $f : \mathbb{R}^N \to \mathbb{C}^m$ with $m \leq c\left(\frac{w(S_{\mathcal{M}})}{\epsilon}\right)^2$.
- Theorem 2.1 bounds $S_{\mathcal{M}}$.
- Apply both theorems to complete proof.

□